Supplementary Information to:

Carbon emissions along divergent plate boundaries modulate icehouse-greenhouse climates

by Ben R. Mather[1], R. Dietmar Müller[2], Adriana Dutkiewicz[2], Sabin Zahirovic[2]

[1] – School of Geography, Earth and Atmospheric Sciences, The University of Melbourne, VIC 3010, Australia
[2] – EarthByte Group, School of Geosciences, The University of Sydney, Sydney, NSW 2006, Australia
* Corresponding author: ben.mather@unimelb.edu.au

Parameter	**Symbol**	**Units**	**Ref value**	**Value**	**A**	**B**	**C**
Half-spreading rate	*u*	cm/a	3	varies	0.881	0.262	
Compaction length	*d*	log10 km	1.5044	1.5044		0.359	
Potential temperature	*T*	°C	1350	1350		-2.91×10^{-4}	
Fertility	*c*	wt. %	19	19		7.50×10^{-3}	
Volatile content	*v*	wt ppm	100	150		5.40×10^{-3}	0.714

Supplementary Table 1. Coefficients and reference values for calculating the flux of water into the bottom of new oceanic mantle lithosphere at mid-ocean ridges[32].

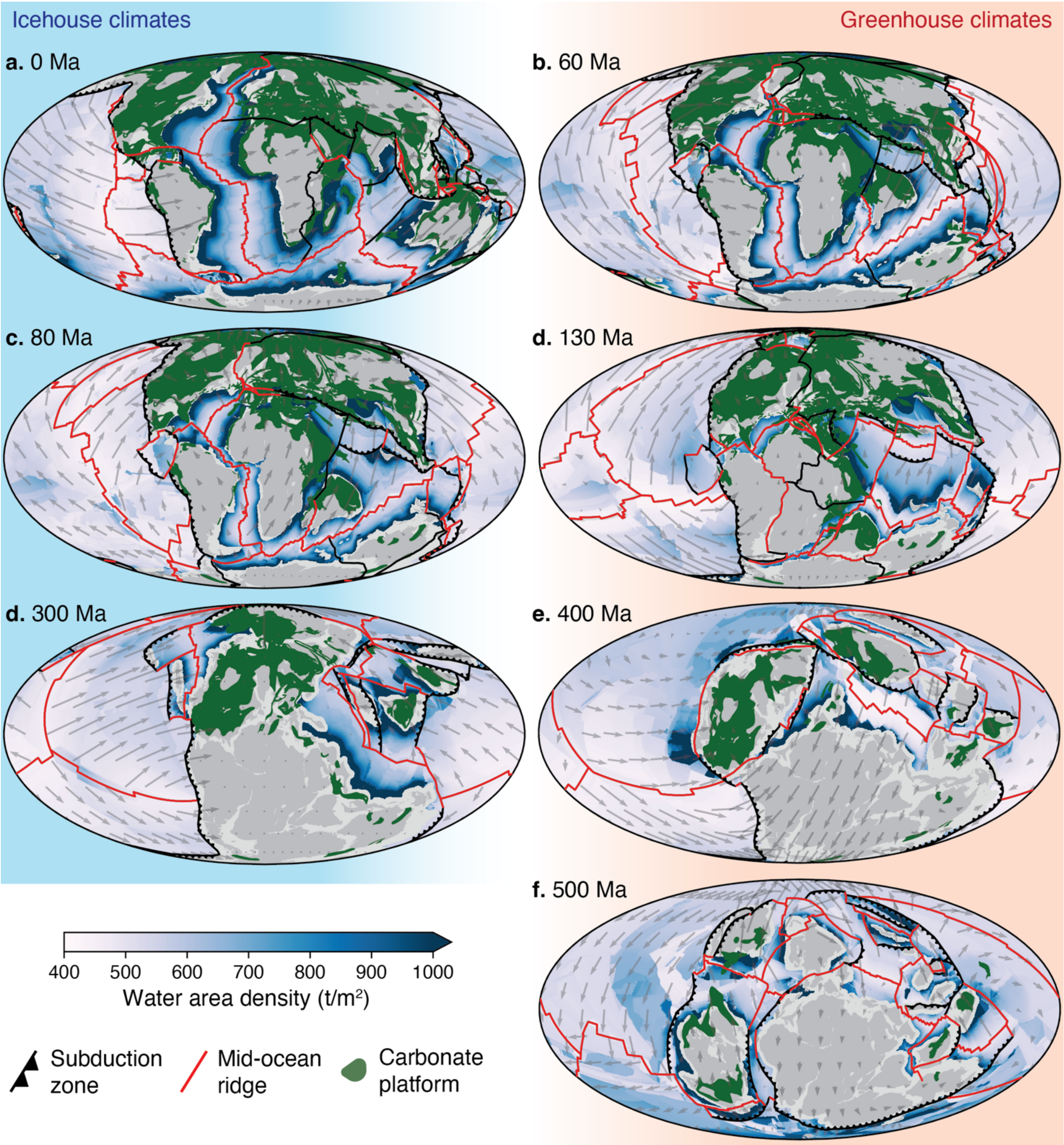

Supplementary Figure 1. Total concentration of water in oceanic plates reconstructed through major icehouse–greenhouse climates. The density of water contained within the oceanic plates (in tonnes per metre squared) corresponds to the timeseries in Figure 2.

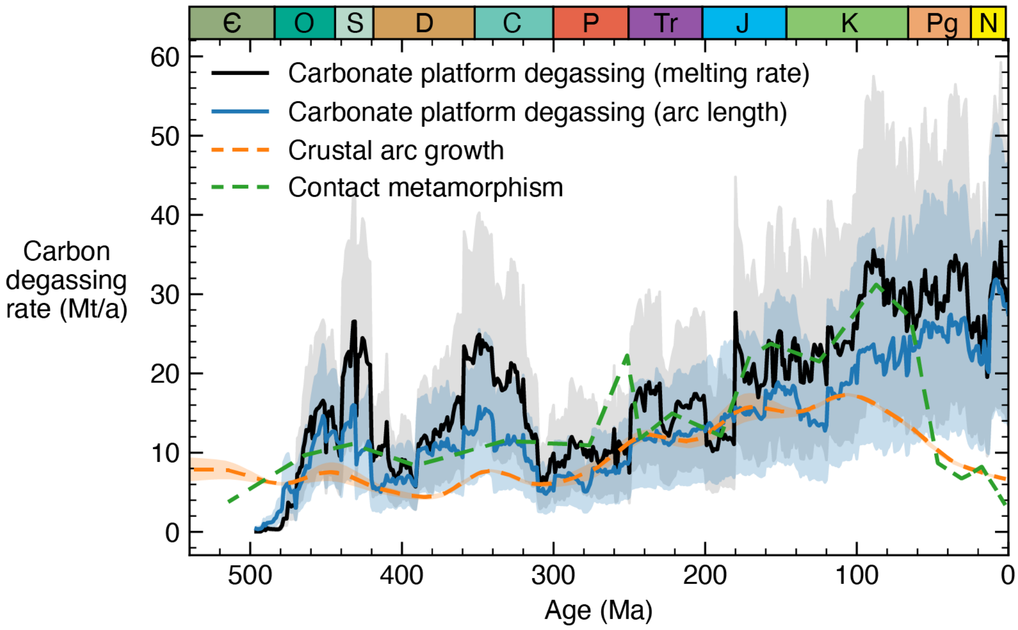

Supplementary Figure 2. Rates of carbonate platform degassing along volcanic arcs. The degassing rate is calculated by scaling the present-day carbonate platform outflux (13.4–44.5 Mt C/a)[9] against the melting rate[23] (black line) and arc length (blue line). The linear carbon outflux trend holds if we scale the carbon loss at carbonate platforms by intersecting arc length to be consistent with previous studies[20] (Figure 2). The "crustal arc growth" curve is based on arc magma addition rates[24] scaled by the total arc length[4] (dashed orange line). The "contact metamorphism" curve represents an alternative model of carbonate platform outflux due to contact metamorphism[12], which is scaled by zircon populations.

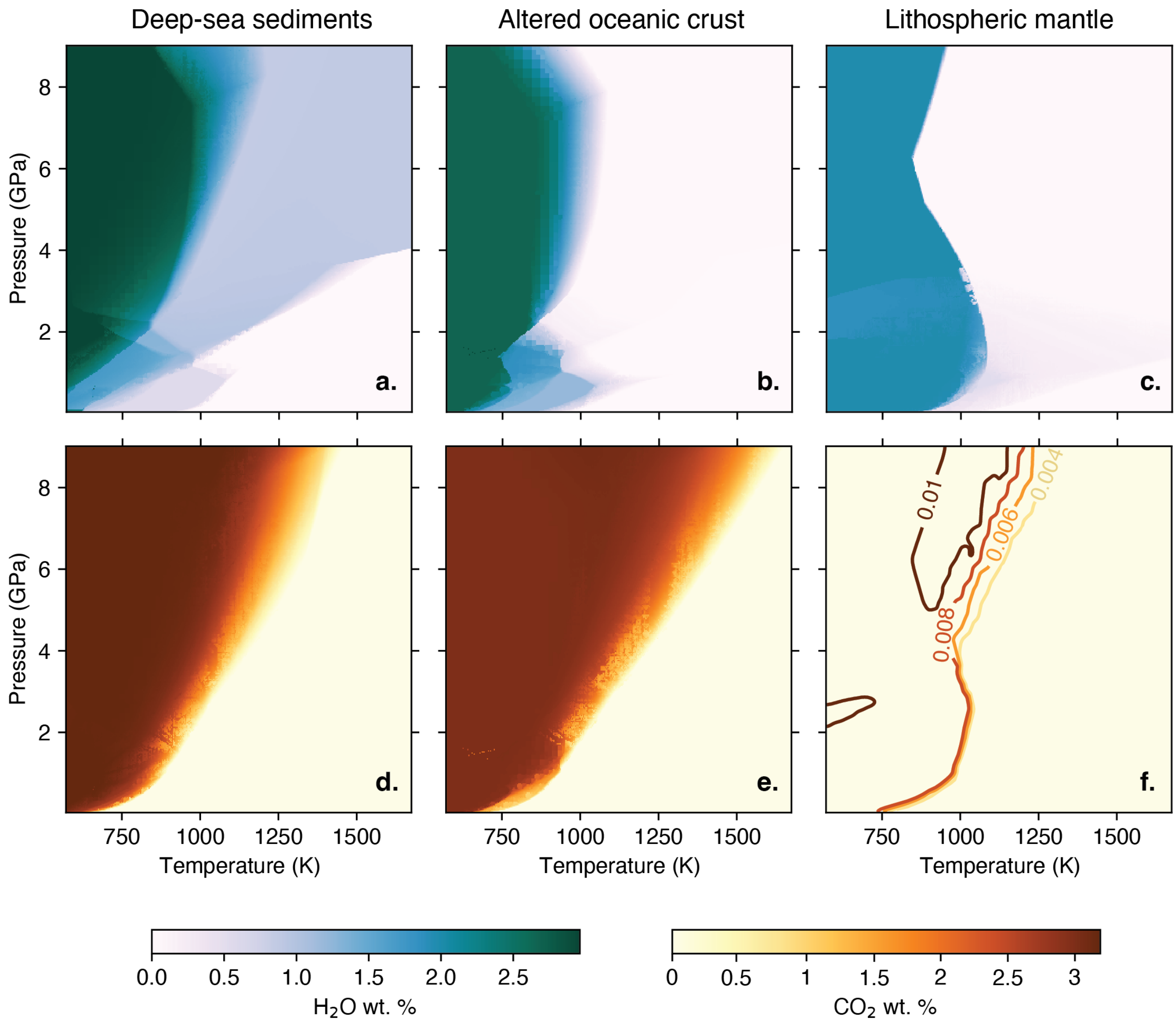

Supplementary Figure 3. H_2O and CO_2 concentration of volatile-carrying reservoirs over a range of pressure and temperature. Phase diagrams were calculated using Perple_X[18] and are identical to those published in a previous study[7]. The concentration of H_2O (**a**-**c**) and CO_2 (**d**-**f**) were extracted across a range of upper mantle temperature and pressure conditions to determine the loss of water and carbon at sub-arc depths. Panel **f.** is contoured by the wt. % of CO_2 because it is orders of magnitude smaller than deep-sea sediments (**d**) or altered oceanic crust (**e**).

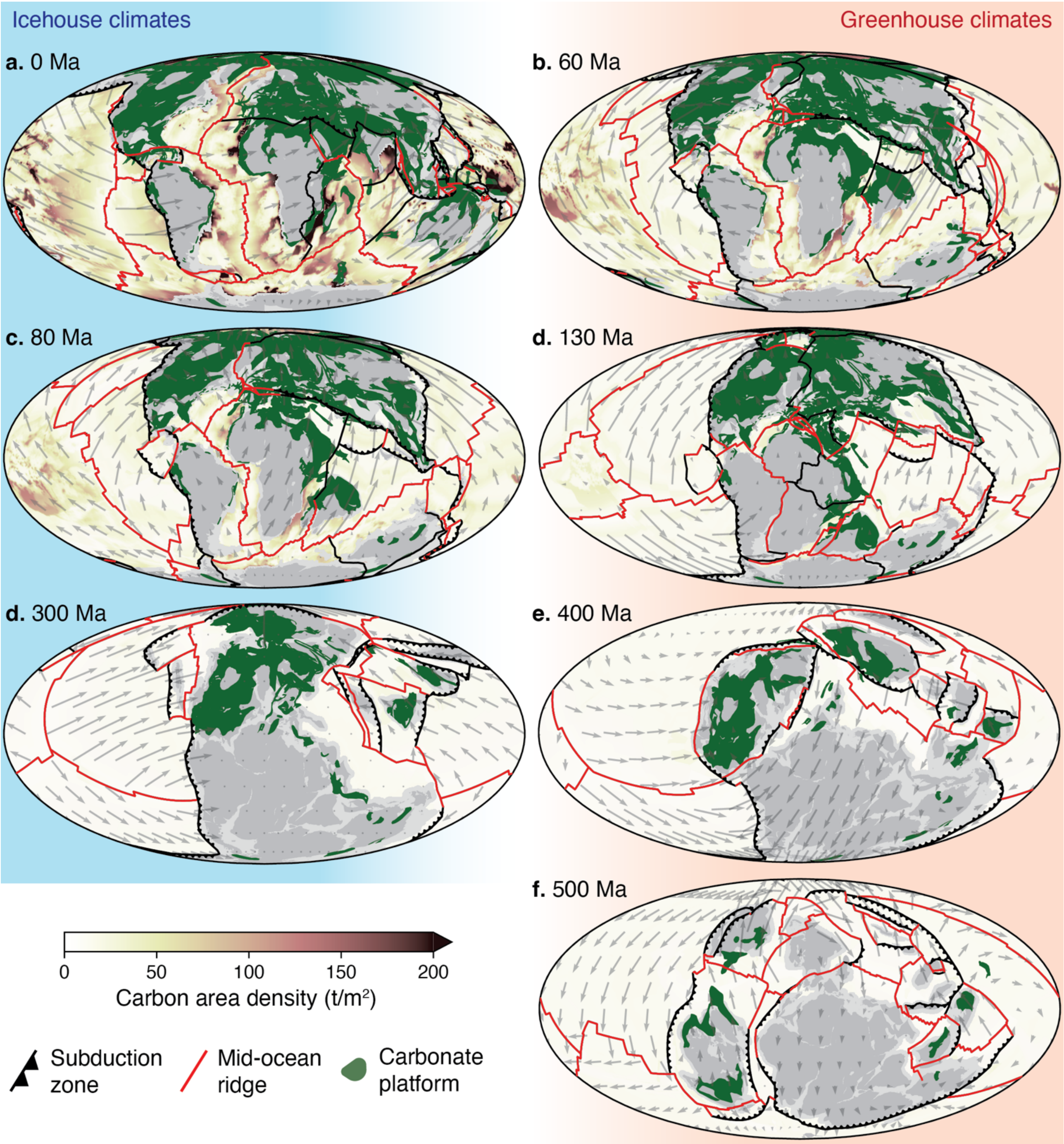

Supplementary Figure 4. Total concentration of carbon in oceanic plates reconstructed through major icehouse–greenhouse climates. The density of carbon contained within the oceanic plates (in tonnes per metre squared) corresponds to the timeseries in Figure 2.

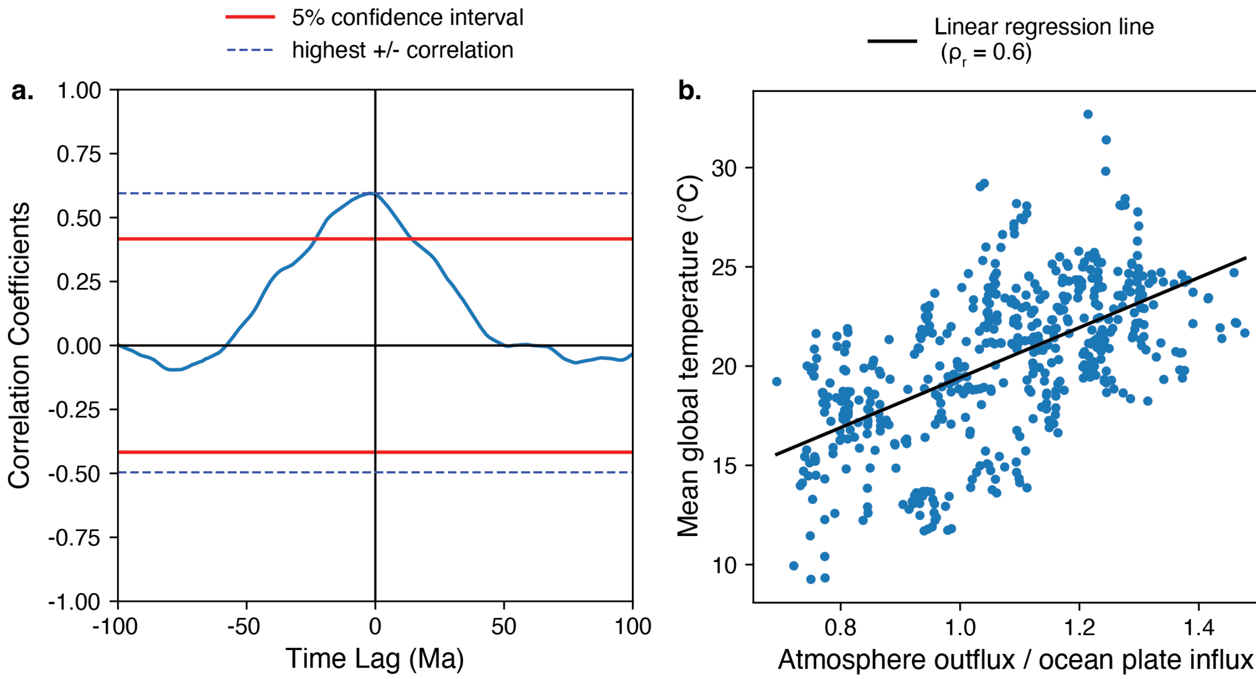

Supplementary Figure 5. Statistical relationship between atmosphere outflux / subduction influx ratio and mean global temperature. a. the cross correlation examines the phase offset between the two signals. The strongest correlation (ρ_r = 0.6) occurs for zero time offset, which indicates the ratio of carbon outflux to subduction influx is synchronised with global temperature (to within a maximum temporal of 1 Myr). **b.** Plot of mean global temperature[37] against the ratio of atmosphere outflux to subduction influx. A linear regression line through the data has a Pearson correlation coefficient, ρ_r, of 0.6.

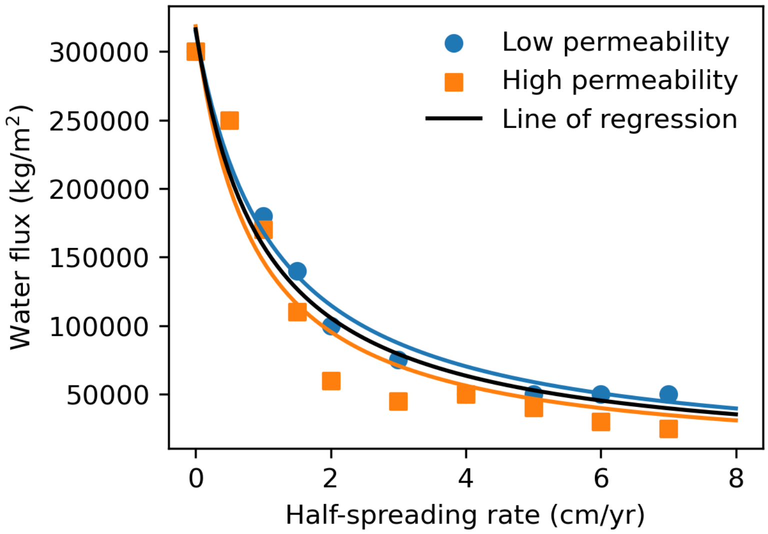

Supplementary Figure 6. Relationship between water outflux and half-spreading rates at mid-ocean ridges. A reciprocal function was fitted to low and high permeability data on mantle hydration and hydrothermal circulation at MORs[2] (refer to Methods). This relationship is applied to MOR segments in the plate model to estimate the water flux back through geological time.